Journal of Glaciology

IGS

Paper

*We dedicate this publication to Prof. H.R. von Gunten, a pioneer in the development of ^{210}Pb applications in environmental research, upon his 90th birthday.

Cite this article: Gäggeler HW, Tobler L, Schwikowski M, Jenk TM (2020). Application of the radionuclide ^{210}Pb in glaciology – an overview. *Journal of Glaciology* **66**(257), 447–456. https://doi.org/10.1017/jog.2020.19

Received: 3 December 2019
Revised: 2 March 2020
Accepted: 3 March 2020
First published online: 13 April 2020

Key words:
mountain glaciers; ice core; ice chronology/dating; glaciological instruments and methods; accumulation

Author for correspondence:
Theo M. Jenk, E-mail: theo.jenk@psi.ch

cambridge.org/jog

Application of the radionuclide ^{210}Pb in glaciology – an overview*

Heinz W. Gäggeler[1,2], Leonhard Tobler[1], Margit Schwikowski[1,2,3] and Theo M. Jenk[1,3]

[1]Laboratory for Environmental Chemistry, Paul Scherrer Institut, 5232 Villigen, Switzerland; [2]Department of Chemistry and Biochemistry, University of Bern, 3012 Bern, Switzerland and [3]Oeschger Centre for Climate Change Research, University of Bern, 3012 Bern, Switzerland

Abstract

^{210}Pb is an environmental radionuclide with a half-life of 22.3 years, formed in the atmosphere via radioactive decay of radon (^{222}Rn). ^{222}Rn itself is a noble gas with a half-life of 3.8 days and is formed via radioactive decay of uranium (^{238}U) contained in the Earth crust from where it constantly emanates into the atmosphere. ^{210}Pb atoms attach to aerosol particles, which are then deposited on glaciers via scavenging with fresh snow. Due to its half-life, ice cores can be dated with this radionuclide over roughly one century, depending on the initial ^{210}Pb activity concentration. Optimum ^{210}Pb dating is achieved for cold glaciers with no – or little – influence by percolating meltwater. This paper presents an overview which not only includes dating of cold glaciers but also some special cases of ^{210}Pb applications in glaciology addressing temperate glaciers, glaciers with negative mass balance, sublimation processes on glaciers in arid regions, determination of annual net snow accumulation as well as glacier flow rates.

Introduction

^{210}Pb has a half-life of 22.3 years and is a member of the natural decay series of ^{238}U. This actinide nuclide exists in the Earth continental crust at a level of ~1.7 ppm (Wedepohl, 1995). One of the progenies of ^{238}U is ^{222}Rn, a radioactive isotope of the noble gas radon, which emanates from the soil into the atmosphere. Due to its half-life of 3.8 days, ^{222}Rn is transported within the lower troposphere over large distances and altitudes (Feichter and Crutzen, 1990; Lee and Feichter, 1995). There, ^{222}Rn decays via short-lived nuclides (half-lives shorter than 30 min) to ^{210}Pb. All progenies of ^{222}Rn are heavy metals and attach to aerosol particles predominantly from the accumulation mode (diameters between ~100 and 300 nm). Thereafter, the behavior of ^{210}Pb in the atmosphere is identical to that of aerosol particles. The atmospheric residence time of ^{210}Pb is in the order of weeks (Kuroda and others, 1978), with a trend to longer values for higher altitudes (Moore and others, 1973). ^{210}Pb then decays via ^{210}Bi (a β-emitter with a half-life 5 days) to ^{210}Po (an α-emitter with a half-life of 138 days) to stable ^{206}Pb. ^{210}Pb is usually deposited on the Earth surface with precipitation except for very arid regions where dry deposition becomes dominant. Commonly two models are applied that describe ^{210}Pb deposition, constant initial concentration (CIC) and constant rate of supply (CRS). In glaciology, usually the CIC assumption best describes the behavior because archived ^{210}Pb in glaciers simply reflects the precipitation history with no secondary processes involved. From environmental monitoring it is well known that the ^{210}Pb activity concentrations in air at a given site – and therefore also in fresh precipitation at this site – is quite constant over time on an annual basis (Gäggeler, 1995). This is different for e.g. lake sediments where the recorded ^{210}Pb activity concentration is modulated by numerous environmental processes prior to deposition in the sediment. In this case, the CRS assumption often holds best (Appleby and Oldfield, 1978; Appleby, 2008). ^{210}Pb application in glaciology has been pioneered in the 1960s by G. Cozaz from the group of E. Picciotto (Université Libre de Bruxelles, Belgium). She analyzed snow and ice samples from Antarctica (Crozaz and others, 1964), Greenland (Cozaz and Langway, 1966) and from the European Alps (Crozaz, 1967). A more general overview on early ^{210}Pb applications in environmental research can be found in Goldberg (1963).

The activity concentration of ^{210}Pb in the lower troposphere over Europe amounts to ~0.2–0.7 mBq m^{-3} (Gäggeler and others, 1995). In Polar regions, the values are significantly lower, for example 0.015 mBq m^{-3} at Franz Joseph Island or 0.013 mBq m^{-3} at the South Pole (Rangarajan and others, 1986). Moreover, there is a decrease in activity as a function of altitude (Turekian and others, 1977; Balkanski and others, 1993). Model calculations showed that the ^{210}Pb activity concentration of ground-level air has a strong geographical pattern with significantly lower values over the oceans compared to coastal or continental sites (Feichter and Crutzen, 1990). This simply reflects the pattern of the ^{238}U concentrations, the source of ^{222}Rn, which are almost three orders of magnitude lower in ocean water compared to soil with 3 ppb and 1.7 ppm, respectively (Mason and Moore, 1982). No significant seasonal variability in the ^{210}Pb activity concentrations in air from Fribourg (Switzerland) or Munich (Germany) was found (Gäggeler, 1995), with an average value of ~0.5 mBq m^{-3}. In contrast, at higher altitude, for example at the Jungfraujoch (3450 m a.s.l., Switzerland), a pronounced seasonal dependence in the ^{210}Pb activity concentrations was observed with typical values of

0.6 mBq m^{-3} in summer and 0.05 mBq m^{-3} in winter (Gäggeler and others, 1995). The reason is the strong convective vertical mixing in summer (Baltensperger and others, 1991).

The determination of ^{210}Pb in environmental samples is usually performed either via γ-counting (46 keV line) or via measurement of its grand-daughter ^{210}Po via α-counting (5.3 MeV α-line). γ-Counting is restricted to samples with rather high activity concentrations of ^{210}Pb due to the high conversion of the low energy γ-line at 46 keV (96% in the form of electron and only 4% in the form of γ emission), but also due to a rather low efficiency of γ-detectors. γ-Counting enables measurements without any chemical treatment and is usually applied for lake sediments (Gäggeler and others, 1976) or peat bogs but not for precipitation or ice samples.

In this overview, we focus on ^{210}Pb activity measurements in firn and ice samples using α-counting of its grand-daughter ^{210}Po. Prerequisite of this approach is the secular equilibrium between ^{210}Pb and ^{210}Po, which is reached after ~1½ years. This corresponds to four half-lives of the grand-daughter nuclide ^{210}Po ($T_{½}$ = 138 days) when 94% of saturation with equal activity of ^{210}Pb and ^{210}Po is reached.

Experimental procedure

The procedure to extract ^{210}Po from snow and ice samples is rather simple: under reducing conditions, polonium spontaneously deposits onto the surface of a silver plate immersed into the melted sample (Gäggeler and others, 1983). Before melting of a sample of ~100–200 mL of water, 50 mL HCl_{conc} is added as well as 100 µL of a ^{209}Po standard with known activity. The solution is then heated to 90°C for ~10 h. Reducing condition is established by bubbling SO_2 gas through the liquid for 3 min. A silver disk of typically 6 mm diameter is immersed into the liquid that is continuously mixed with a magnetic stirrer. In order to prevent polonium deposition on both sides of the silver plate, it is advisable to mount the plate into a plastic frame that protects deposition on the back side (Gäggeler and others, 1983). After deposition, the silver plate is placed opposite to a silicon semiconductor detector, able to measure energy-resolved α-particles.

To reach a detection uncertainty of 1%, 10 000 counts are required. The ^{209}Po standard, which is added to the sample prior to the polonium extraction, is used to determine the polonium deposition and overall yield. ^{209}Po has an α-decay energy of 4.9 MeV, which is well separated from the 5.3 MeV α-line from ^{210}Po. Yields are typically ~80% and the detection limit of this counting technique is ~1 mBq kg^{-1} for a sample size of ~200 g and a counting time of 1 week. A typical example of an α-spectrum of a sample from Chongce Ice Cap (Tibet, China) is depicted in Figure 1 (Hou and others, 2018), showing the two α-lines from ^{209}Po and ^{210}Po.

^{210}Pb activity concentrations on glacier surfaces

The mean annual activity concentration of ^{210}Pb in precipitation at München-Neuherberg (Germany) is ~150 mBq L^{-1} and the annual deposition rate is 130 Bq m^{-2} (Hötzl and others, 1983). In Fribourg, Switzerland, the activity concentration is somewhat smaller, ~50 mBq L^{-1} (Steinmann and others, 2015). Table 1 summarizes ^{210}Pb activity concentrations of surface samples from different glaciers worldwide.

Generally, the variation and differences in the levels of ^{210}Pb activity concentrations in the freshly deposited snow/ice observed for the different regions are as expected, considering the regional emission source strength of the ^{210}Pb precursor: crustal ^{238}U. ^{238}U concentrations are much lower in ocean water compared to soil

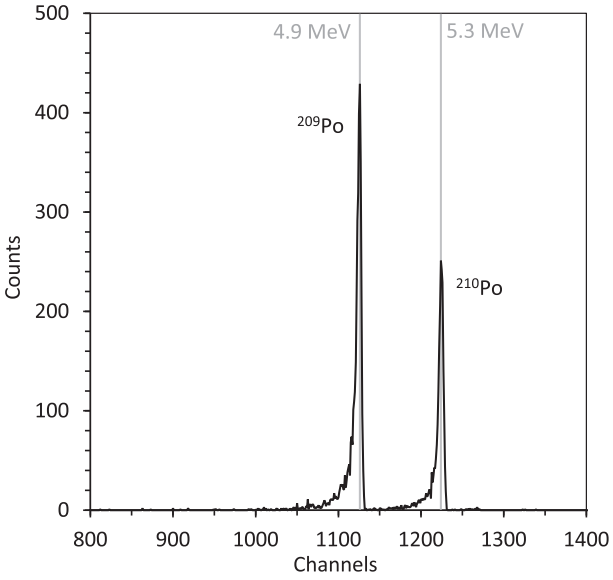

Fig. 1. α-Spectrum of a surface sample (103 g) from Chongce Ice Cap (Tibet, China) measured for 241 844 s with a surface barrier detector. The α-lines of ^{209}Po (standard) and ^{210}Po (sample) have energies of 4.9 and 5.3 MeV, respectively.

which may further be rich or poor in its uranium deposits (Mason and Moore, 1982). ^{210}Pb activity concentrations are lowest at Polar sites (Table 1, Index a), both from Antarctica and the Arctic. The average value is ~30 mBq kg^{-1}. It is interesting to note that across the European Alps (b) the ^{210}Pb activity concentrations are rather similar, on average 86 ± 16 mBq kg^{-1}. The most continental sites listed in Table 1 are from Altai, Tien Shan (c) and certain areas of the Tibetan Plateau (Chongce). At these locations, the highest values of ^{210}Pb activity concentrations were observed.

Values of the activity concentrations in the Andes (d) are lower for sites affected predominantly by marine air masses related to the prevailing Westerlies (Cerro Tapado, Mercedario) but also for Pio XI in Patagonia. They are higher for sites under influence of continental air masses related to the tropical circulation (Chimborazo, Corupuna, Illimani, and surprisingly, as found by Vimeux and others (2008), also for the Patagonian site San Valentin). On average, however, they are rather similar to those from the European Alps. Significant differences are also observed between the sites in the Himalaya (e). This may reflect the influence of the monsoon. Sites that are heavily influenced by monsoon, such as Changme-Kangpu and Nehnar Changme, show lower values while at the continental site Chongce in Tibet the value is significantly higher. Rather unexpected are the high ^{210}Pb activity concentrations for glaciers in the Mount Cook area in New Zealand considering the fact that these glaciers are in close vicinity to the Tasman Sea, the source of precipitation. We attribute these rather surprisingly high values to air mass transport from Australia. It is well known that Australian geology is rich in uranium deposits, resulting in many uranium mining sites, and is therefore a strong source of ^{222}Rn, the precursor of ^{210}Pb. The study by Marx and others (2005) using ^{210}Pb as a monitor of Australian dust flux into New Zealand strongly corroborates the above interpretation for the observed high values.

Seasonality of ^{210}Pb deposition

Due to vertical convective mixing within the atmosphere during summer, strong seasonal variability in the ^{210}Pb activity concentrations in fresh snow may result. As an example, Figure 2 depicts highly resolved ^{210}Pb activity concentrations at Grenzgletscher (4200 m a.s.l., Switzerland) (Eichler and others, 2000). The

Table 1. ^{210}Pb activity concentrations in surface snow/ice as reported in the literature or deduced from therein-presented profiles by extrapolation to zero depth

Index	Region	Site	mBq kg^{-1}	Reference
(a)	Polar (Antarctica)	South Pole	28	Crozaz and others (1967)
	Polar (Antarctica)	Base Roi Baudoin	21	Crozaz and others (1967)
	Polar (Antarctica)	South Pole	32	Sanak and Lambert (1977)
	Polar (Antarctica)	Taylor Dome	20	Morse and others (1999)
	Polar (Antarctica)	Dome Fuji	32	Suzuki and others (2004)
	Polar (Antarctica)	Allan Hills	16	Dadic and others (2015)
	Polar (Greenland)	Camp Century	47	Crozaz and Langway (1966)
	Polar (Greenland)	various sites	15–23	Dibb (1990)
	Polar (Greenland)	Dye 3	40	Dibb and others (1993)
	Polar (Svalbard)	Lomonosovfonna	30	Pinglot and others (2003)
	Polar (Svalbard)	Lomonosovfonna	35	Wendl and others (2015)
	Polar (Canada)	Agassiz Ice Cap	44 ± 19	Peters and others (1997)
(b)	Europ. Alps (France)	Dome du Goûter	≈100	Vincent and others (1997)
	Europ. Alps (Switzerland)	Grenzgletscher	85	Eichler and others (2000)
	Europ. Alps (Switzerland)	Colle Gnifetti	67	Gäggeler and others (1983)
	Europ. Alps (Switzerland)	Jungfraujoch	67	Schotterer and others (1977)
	Europ. Alps (Switzerland)	Silvretta	≈100	Pavlova and others (2015)
	Europ. Alps (Italy)	Ortles	110	Gabrieli and others (2016)
	Europ. Alps (Austria)	Vernagtferner	83	von Gunten and others (1982)
	Europ. Alps (Austria)	Kesselwandferner	72	Picciotto and others (1967/68)
(c)	Altai (Russia)	Belukha	≈280	Olivier and others (2006)
	Altai (Mongolia)	Tsambagarav	272	Herren and others (2013)
	Tien Shan (China)	Miaoergou	≈400	Wang and others (2014)
(d)	Andes, Patagonia (Chile)	Pio XI	≈10	Schläppi (2010)
	Andes, Patagonia (Chile)	San Valentin	103	Vimeux and others (2008)
	Andes (Chile)	Cerro Tapado	43[a]	Ginot and others (2006)
	Andes (Argentina)	Mercedario	33	previously unpublished data
	Andes (Bolivia)	Illimani	106	Knüsel and others (2003)
	Andes (Peru)	Coropuna	130	previously unpublished data
	Andes (Ecuador)	Chimborazo	60	previously unpublished data
(e)	Sikkim (India)	Changme-Kangpu	113	Nijampurkar and others (1985)
	Kashmir (India)	Nehnar Changme	70	Nijampurkar and others (1993)
	Tibet (China)	Geladaindong	89[a]	Kang and others (2015)
	Tibet (China)	Chongce	236	Hou and others (2018)
(f)	Mount Cook area (New Zealand)	Annette Plateau	132	Gäggeler and others (2011*a*)
	Mount Cook area (New Zealand)	Hutton glacier	132	Gäggeler and others (2011*b*)
	Mount Cook area (New Zealand)	Baker glacier	172	Gäggeler and others (2011*b*)

This table is structured according to different geographical regions: (a) Polar, (b) European Alps, (c) very continental sites such as Altai, and Tien Shan, (d) Andes and Patagonia (e) Indian and Chinese Himalaya and (f) the New Zealand Mount Cook area. When not available from the literature, values are activity concentrations at zero depth deduced from extrapolations of depicted data as a function of depth. No uncertainties are listed. They are typically 10–20%, caused by the variability in the results from individual measurements and not by counting statistics.
[a]Extrapolated values after correction for melting and/or sublimation, see Figures 7 and 8 and related sections.

average winter and summer values for this site amount to ~25 and 125 mBq kg^{1}, respectively.

The very low values prove that in winter little exchange of air between the free troposphere and the planetary boundary layer occurs. In principle, it is possible to determine seasonality as well as individual annual deposition rates by such measurements. However, it should be mentioned that ^{210}Pb measurements are time consuming and therefore dating by annual layer counting is much simpler using easy to analyze chemical tracers that also exhibit a high seasonal variability such as for example ammonium (see e.g. Döscher and others, 1995).

Nevertheless, from Figure 2 it becomes evident that ^{210}Pb dating requires longer-term averages (at least annual) to minimize the effect of seasonal fluctuations.

Dating of ice cores with ^{210}Pb

Basic principles

If an ice core should be dated with the ^{210}Pb method several prerequisites need to be fulfilled:

- The CIC assumption should be fulfilled as well as constant annual precipitation rates. This results in a CRS situation.
- Post-depositional effects (melting, sublimation and wind drift) should be minimal.
- In some cases, however, it could be shown that ^{210}Pb activity profiles were not much influenced by percolating meltwater. We assume that the ^{210}Pb atoms are strongly adsorbed on the surfaces of mineral dust particles contained in the ice matrix (see section '^{210}Pb dating of temperate glaciers').
- A great advantage is the fact that sampling can be made from the outside of the core, which is usually not suited for chemical trace analysis.
- Continuous sampling is essential – though at low sample resolution.
- Measurements should be continued to depths where constant values are reached. These indicate the natural background level needed for background correction.
- With the surface age known (equal to the date of drilling), a fit through the data plotted against depth in meter water equivalent (m w.e., converted from depth in meter by multiplying with density to account for snow/firn densification as observed in the measured density profile) yields the final age–depth relationship by applying the radioactive decay law:

$$t = \frac{-s}{\ln(2)} \cdot T_{1/2} \cdot x, \quad (1)$$

where t is the age in years since the drill date, s is the slope of the fit, $T_{½}$ is the half-life of ^{210}Pb (22.3 years) and x is the depth in

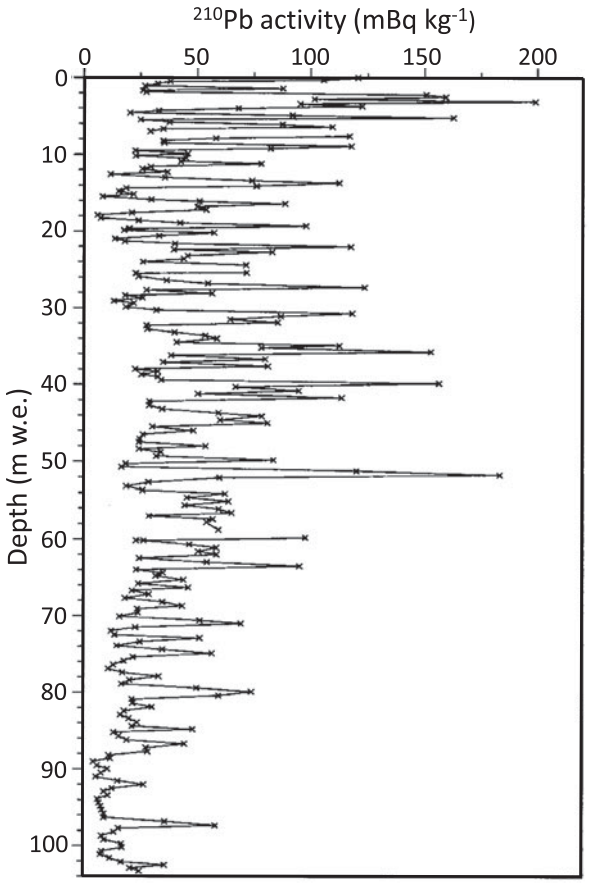

Fig. 2. Highly resolved depth profile of ^{210}Pb activity concentrations in an ice core from Grenzgletscher (4200 m a.s.l., Switzerland). Maximum and minimum values represent summer and winter precipitation, respectively. Figure from Eichler and others (2000). Reprinted from *Journal of Glaciology* with permission of the International Glaciological Society.

m w.e. From the uncertainty of the regression slope, the dating uncertainty can be estimated (see Fig. 3). Note that the uncertainty bands are different if the fit relates either to the scale of the measured ^{210}Pb concentration activity or to the therefrom-deduced age scale. This is because, for the latter case, the uncertainty is zero at the surface for which the age is known precisely, that is equal to the year of drilling.

Figure 3 shows an example of ^{210}Pb measurements of an ice core from Belukha (Olivier and others, 2006). After the expected exponential decrease with depth or time, respectively, the values reach a plateau, indicating an average background value of 3.6 ± 1.2 mBq kg^{-1} (value already corrected for the small instrumental background of ~1 mBq kg^{-1}, see section 'Experimental procedure'). This value represents ^{210}Pb from mineral dust contained in the ice. This activity is called supported ^{210}Pb. The background value observed at Belukha is typical for many glacier sites. Note that this natural background value has always to be subtracted from all the measured ^{210}Pb activity concentrations to deduce the final dating (Fig. 3b).

The time range accessible with the ^{210}Pb method depends on the initial activity concentration at the surface and the respective background. The dating time frame is ~80 years for sites with ~40 mBq kg^{-1} surface activity concentration and increases to ~180 years for the most continental sites such as Tien Shan (400 mBq kg^{-1}) or Belukha (280 mBq kg^{-1}), respectively. From Figure 3b it becomes clear that the dating uncertainty increases as a function of age (in Fig. 3b about ±10 years for the lowermost samples from the mid-19th century). Advantage of the ^{210}Pb dating is that it is independent from other approaches such as annual layer counting based on chemical tracers.

Effect from thinning of annual layers

Ice is a plastic solid, therefore increasing pressure induced by overlaying ice layers causes horizontal glacier flow, resulting in a reduction of the original ice layer thickness. This effect is called thinning and becomes significant particularly for deeper ice core sections. Consequently, a deviation of the exponential trend in the ^{210}Pb activity concentration with depth is expected. Several mathematical models describe such a thinning. We use here the oldest, original one by Haefeli (1961) to illustrate the basic principle of this effect. This model describes the time as a function of

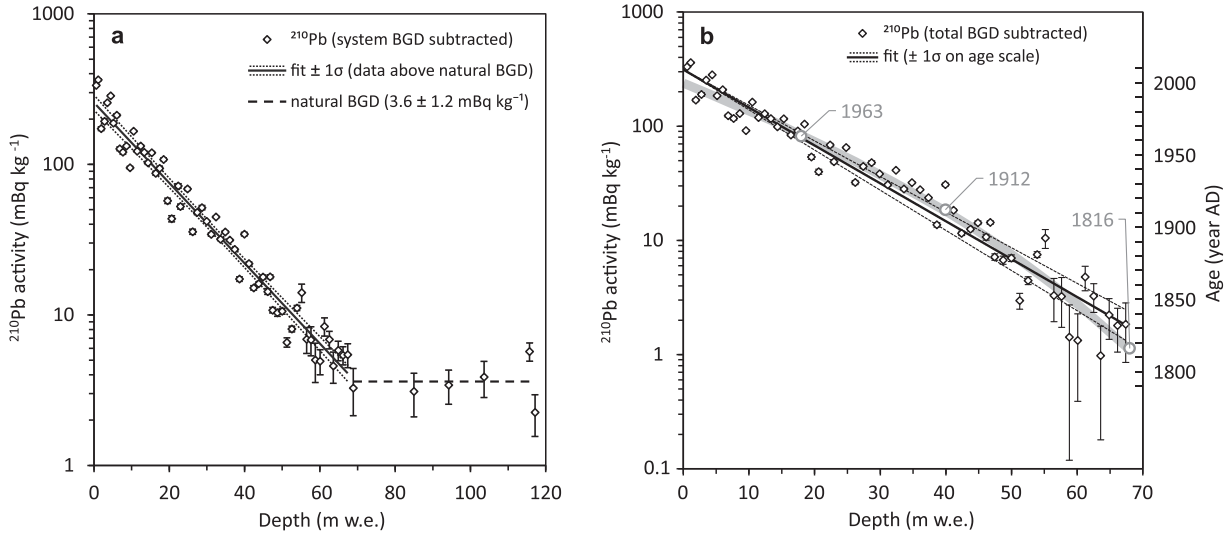

Fig. 3. ^{210}Pb activity concentration and derived age as a function of depth in an ice core from Belukha. (a) ^{210}Pb activity concentration as a function of depth. The thin dotted line indicates the 1σ uncertainty band of the regression fit. The dashed line indicates the average value for the lowermost samples reflecting the input from supported ^{210}Pb, that is the natural background determined for this site. (b) The same data of ^{210}Pb activity concentration, but with the natural background (supported ^{210}Pb) subtracted, together with the derived age scale as shown on the right *y*-axis as a function of depth. The dotted lines indicate the 1σ dating uncertainty, derived by error propagation, which includes the uncertainty of the regression fit shown in (a). Open gray circles indicate distinct time horizons found in the ice core (^{3}H peak in 1963 from nuclear weapons testing and signals in sulfate related to the known volcanic eruptions from Katmai and Tambora in 1912 and 1815/16, respectively). The fit shown by the thick gray line does account for glacier thinning (see section 'Effect from thinning of annual layers'). Data from Olivier and others (2006).

depth with

$$t = \frac{H}{a}\ln\left(\frac{H}{H-x}\right), \quad (2)$$

where t is the time in years after deposition, H the ice thickness in m w.e., a the net annual accumulation rate in m w.e. and x is the depth from the surface in m w.e.

If this equation is combined with the exponential decay law for ^{210}Pb, the following equation results for the ^{210}Pb activity concentration A as a function of depth (Gäggeler and others, 1983):

$$A = A_0\left(\frac{H}{H-x}\right)^c, \quad (3)$$

with

$$c = -\frac{\lambda H}{a}, \quad (4)$$

where λ is the decay constant of ^{210}Pb (0.0311 a^{-1}).

An example from Colle Gnifetti is shown in Figure 4, highlighting the potential importance to consider the thinning effect when dating by ^{210}Pb. The fit derived based on Eqn (3) accounting for thinning ($R^2 = 0.89$, $n = 13$; residual sum of squares (RSS) = 380.0) is a better description of the observed data than the fit based on the law of exponential decay which does not consider any thinning ($R^2 = 0.85$, $n = 13$; RSS = 557.7).

Special cases

^{210}Pb dating of temperate glaciers

Temperate glaciers are characterized by an ice temperature close to the melting point and the presence of liquid water formed by melting of ice and/or originating from rain or snow melt. Water percolation may therefore influence the ^{210}Pb activity concentration profiles by downward relocation and, in the extreme case, by removal of ^{210}Pb through run-off with meltwater. As an example, Figure 5 shows ^{210}Pb data of an ice core from the temperate Vernagtferner (Austria), with the ice core sampling site located at an elevation of 3150 m a.s.l. (von Gunten and others, 1982).

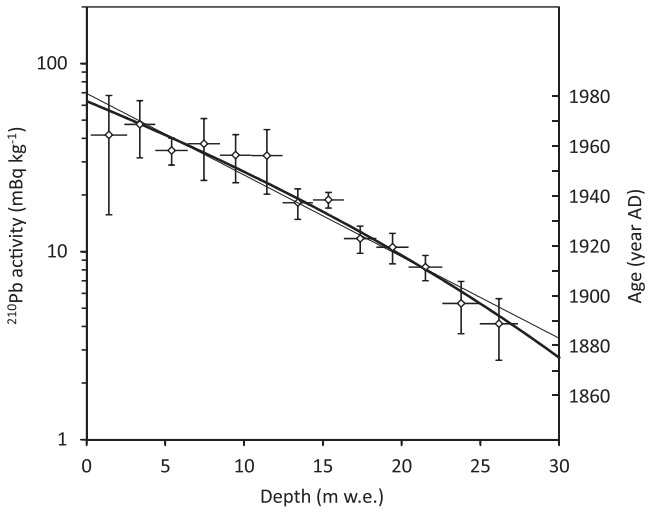

Fig. 4. ^{210}Pb activity concentration as a function of depth in m w.e. at Colle Gnifetti (adapted from Gäggeler and others, 1983). The solid thick line shows a fit through the data accounting for thinning (according to Eqn (2)), whereas the thin line is a fit solely derived from the exponential decay law. Horizontal bars indicate sampling depth ranges and vertical bars the std dev. of the averaged values from individual measurements performed in higher sampling resolution.

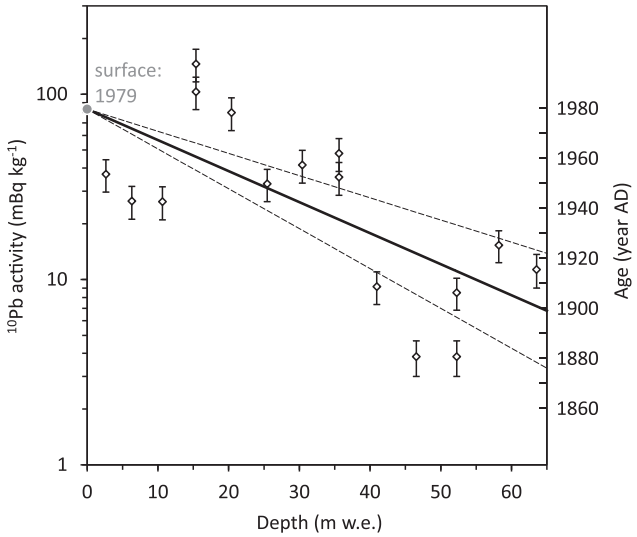

Fig. 5. Continuous ^{210}Pb activity concentration profile in the ice core from the Vernagtferner (3150 m a.s.l., Austria) drilled in 1979 (open symbols with 1σ analytical uncertainty bars). The profile includes three replicate samples. Depicted is a best fit through all ^{210}Pb data. The fit directly relates to the age scale indicated by the right-hand y-axis with the 1σ dating uncertainty shown by the dashed lines. Figure deduced from von Gunten and others (1982).

Obviously, relocation of ^{210}Pb with meltwater resulted in high variability. It is interesting to note that often the maxima of the ^{210}Pb activity concentrations coincide with high levels of mineral dust.

Another example is from the temperate Silvretta Glacier (Switzerland) with the drilling site located at 2927 m a.s.l. (Fig. 6, Pavlova and others, 2015). Again, despite fluctuating ^{210}Pb values, on average the inventory of ^{210}Pb and the exponential decrease looks very reasonable. In this case, the 1963 horizon identified via tritium measurements is predicted slightly older by the ^{210}Pb dating at 1953 but still in agreement within the 1σ uncertainty estimate.

Surface age in case of negative mass balance

Due to climate warming, glaciers in most mountain regions of the world have been retreating and even disappearing at an accelerated rate in recent decades (e.g. Zemp and others, 2015). This increasingly affects also the accumulation areas, for which widespread surface loss is often observed. ^{210}Pb may serve to identify

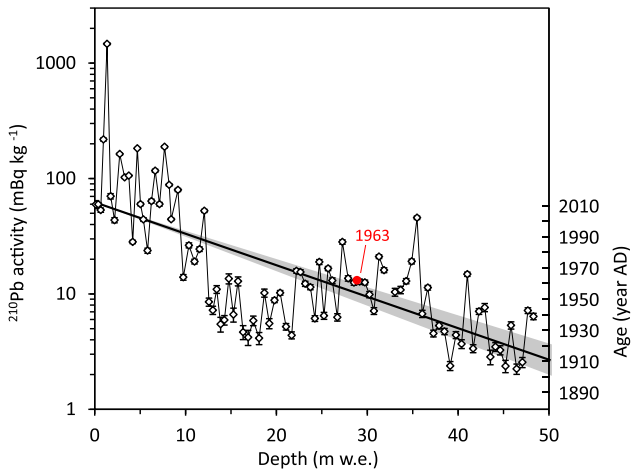

Fig. 6. ^{210}Pb activity concentrations along an ice core from Silvretta, drilled in 2011. The red dot shows the 1963 peak in ^{3}H related to nuclear bomb testing, indicating the accuracy of the dating by ^{210}Pb with uncertainties (1σ) depicted by the shaded area. Adapted from Pavlova and others (2015).

such cases since melting of surface layers may lead to enrichment of ^{210}Pb activity concentrations at the surface. An example is shown in Figure 7 for the Mount Geladaindong Glacier, central Tibetan Plateau (5750 m a.s.l.) (Kang and others, 2015).

In Figure 7, the ^{210}Pb activity concentrations at depths below ~5 m (solid diamonds) follow an exponential decrease. However, the topmost two values (open diamonds) strongly deviate from this trend, seemingly being far too high. We assume that these two data points represent enriched values. The hypothesis is that while matrix water was removed by melting, ^{210}Pb was enriched in the surface layers due to adsorption on rather immobile dust particles. A significant loss of surface mass is corroborated by the presence of the nuclear fallout layer at a shallow depth of only 5.74 m, identified by the prominent peak in the tritium activity concentration (red dot) (Kang and others, 2015). The resulting net accumulation between the date of ice core drilling (October 2005, i.e. surface) and 1963 (at 5.74 m depth) of 14 cm a^{-1} is much smaller than the 30 cm a^{-1} deduced for the lower part of the core from the slope of the exponential decrease (see Fig. 7). A more recent change in the mass balance to negative values thus seems to be a reasonable assumption for this site. Accordingly, the age of the surface can be assumed to differ from the date of drilling (October 2005). The age of the surface was estimated by anchoring the ^{210}Pb profile to the year 1963 represented by the tritium peak at 5.74 m depth, resulting in the time axis depicted on the right *y*-axis. An extrapolation to the surface results in a surface age of 1982 ± 5, hence in a loss of 2005–1982 = 23 ± 5 years of accumulation, and a deduced surface ^{210}Pb activity concentration of 89 mBq kg^{-1} (gray cross), which is a very reasonable value (see Table 1). A final proof of evidence for the validity of the chosen approach can be derived, based on the ^{210}Pb activity concentration observed in the first two values. Under the assumption of surface enrichment, they should reflect the integrated activity of 23 years of ^{210}Pb deposition with the determined initial activity A_0 (89 mBq kg^{-1}). Indeed, the observed high values do account for 81% of the expected activity, suggesting only moderate removal, that is run-off of the deposited ^{210}Pb of ~ 20%. This is in close agreement with the determined preservation of lead in snow and ice under the influence of percolating meltwater of ~70% (Avak and others, 2018, 2019).

Effect of sublimation on the ^{210}Pb profile

Andean glaciers located in the South American dry diagonal are often influenced by strong sublimation. A consequence is the formation of penitents. Sublimation means evaporation of water from the solid phase to the gas phase while non-volatile species such as ^{210}Pb remain in the matrix. Such a situation was extensively studied at Cerro Tapado (30°08′S; 69°55′W; 5534 m a.s.l.) in the Chilean Andes (Ginot and others, 2002, 2006). A large year-to-year variability in loss of H_2O due to sublimation was observed (Ginot, 2001). The sublimation rate was determined by chemical means via measurement of chloride concentrations: at this glacier, most precipitation comes from the nearby Pacific by westerly winds that contains much sea salt. As a consequence, the chloride concentration is rather high and constant in fresh snow. Deviations of the chloride concentration measured in individual ice samples compared to those in fresh snow then yield the enrichment factor due to sublimation. On average, sublimation turned out to result in a mass loss of 60%. This means that a determination of annual net accumulation rates from measured ^{210}Pb profiles differs from total accumulation rates. Figure 8 depicts the situation observed at Cerro Tapado. The trend in the measured chronology of ^{210}Pb activity concentrations as a function of depth indicates an annual accumulation rate of 235 mm w.e. a^{-1} (Fig. 8a). Correcting the ^{210}Pb activity concentration profile by accounting for loss of snow by sublimation using the chloride concentration record (Fig. 8b) results in a revised annual accumulation rate of 405 ± 50 mm w.e., in reasonable agreement with 470 ± 70 mm w.e. from a glaciological estimate (see Ginot, 2001).

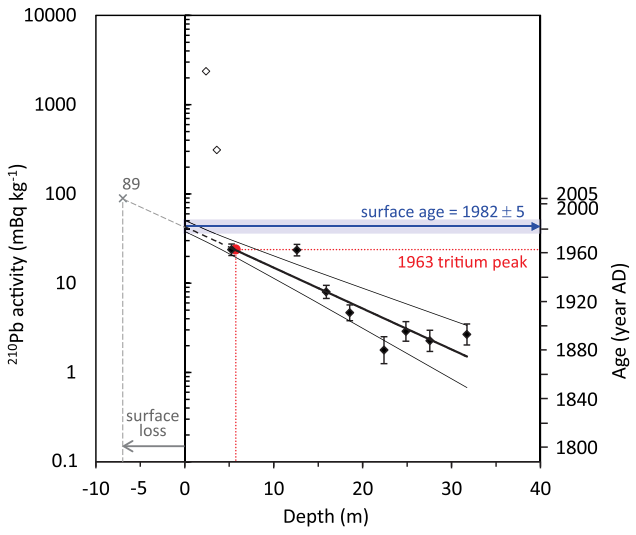

Fig. 7. ^{210}Pb activity concentrations in an ice core from Mount Geladaindong (5750 m a.s.l.) (open and solid diamonds); adapted from Kang and others (2015). For details see text.

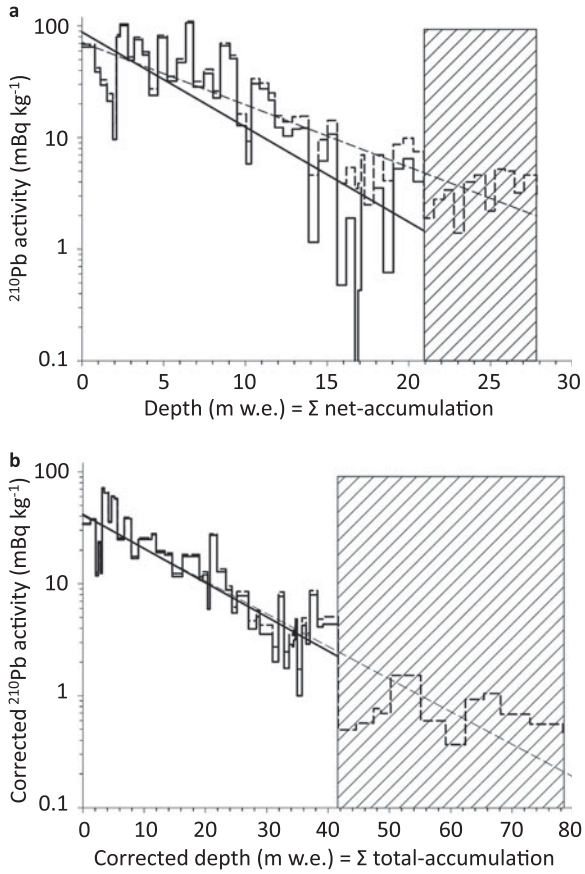

Fig. 8. Effect of sublimation on the ^{210}Pb profile. (a) Measured ^{210}Pb activity concentration in an ice core from Cerro Tapado as a function of depth in m w.e. (b) The same data but here accounting for sublimation resulting in a corrected depth (see text for details). Dashed lines indicate the measured ^{210}Pb activity concentration, and respective trend line. Hatched areas indicate the depth range where ^{210}Pb activity reached the background level from supported ^{210}Pb. The solid lines depict the measured data (and respective trend lines) after substraction of this background (average value within hatched areas). Figure adapted from Ginot and others (2006).

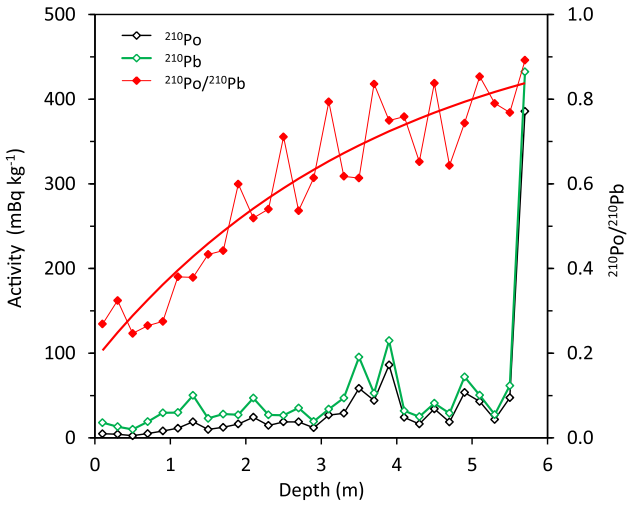

Fig. 9. Activity concentrations of ^{210}Po and ^{210}Pb in a firn core from Jungfraujoch (Switzerland) sampled on 25 March 2007 (reported in Gäggeler and others, 2009). The red line is the modeled fit according to Eqn (5).

Special applications using ^{210}Pb

Determination of the annual deposition rate

At remote sites with no possibility to get meteorological information or to return for stake measurements, the last year's deposition can be determined using the ratio of the grand-daughter radionuclide ^{210}Po and its mother nuclide ^{210}Pb. As stated previously, after ~1½ years the secular equilibrium between these two radionuclides is nearly reached (see Introduction). Between time zero and equilibrium, the relationship between the activity concentrations of ^{210}Po and ^{210}Pb approximately follows the below equation:

$$A_{(^{210}\mathrm{Po})} = A_{(^{210}\mathrm{Pb})}(1 - \mathrm{e}^{(-\lambda t)}), \quad (5)$$

where $A(x)$ is the activity concentration of nuclide x, t is the elapsed time between precipitation date and date of sample collection and λ is the decay constant of ^{210}Po (= ln(2)/138.4 days). Equation (5) is only a close approximation, since the intermediate radionuclide ^{210}Bi the daughter of ^{210}Pb with a half-lie of 5 days is ignored. However, this is justified considering its short half-life compared to those of ^{210}Pb and ^{210}Po, respectively.

Figure 9 depicts an example of this approach for measurements at Jungfraujoch (Switzerland) (Gäggeler and others, 2009). One half of each firn sample was analyzed for ^{210}Po immediately after sampling. The other half was stored for 1½ years and then analyzed again for ^{210}Po, but now representing the ^{210}Pb activity concentration since equilibrium between the two radionuclides was nearly reached. The red curve depicts the ratio between the activity concentrations. The maximum value of 0.84 at 5.7 m depth indicates that the equilibrium at this depth was almost reached already at the time of sample collection (i.e. the time of first analysis). Using Eqn (5), a value for t of 366 days results (i.e. ~1 year) indicating the annual net accumulation at this site to be 5.7 m of snow. Obviously, the same accumulation rate can be deduced from the profile at any other, shallower depth. Therefore, this application is not dependent on the performed sampling depth, which is important to note if intended to be applied at a site with no initial knowledge (although sampling depths covering close to 1 year or more of deposition is favorable to obtain a better constrained fit and accordingly better precision and accuracy for the finally determined accumulation).

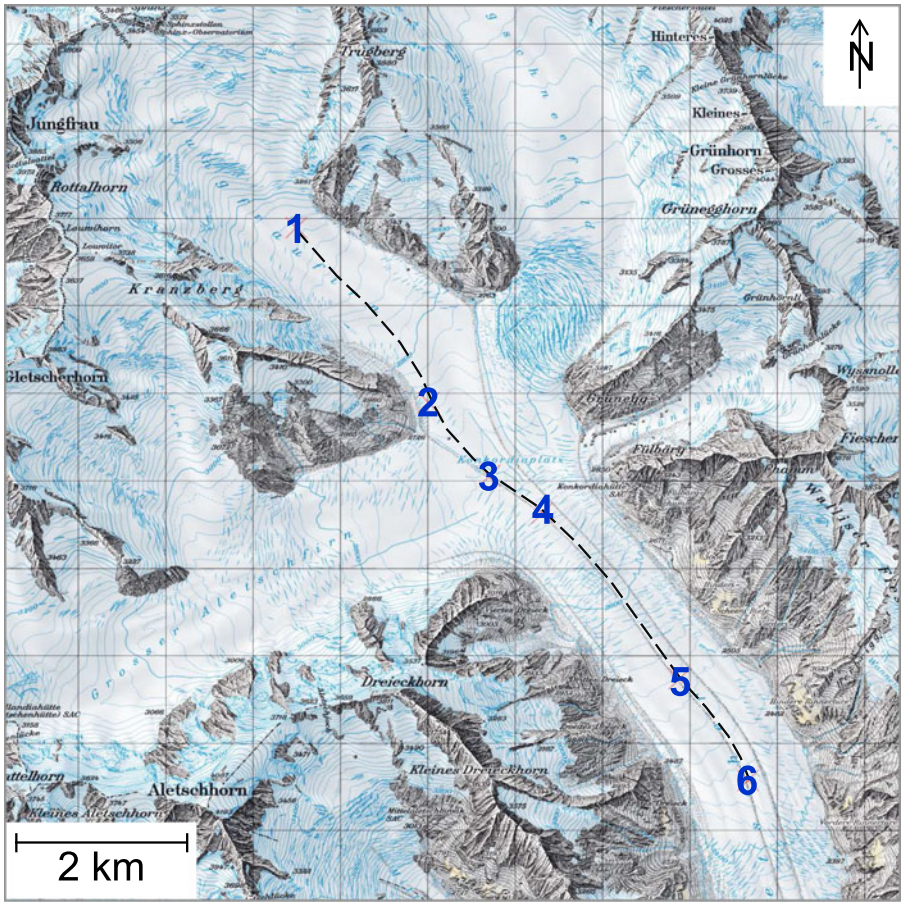

Fig. 10. Trajectory along the Jungfraufirn/Aletsch Glacier (Switzerland) along which surface ice samples were collected for ^{210}Pb analysis. Map reproduced by permission of swisstopo (JA100121).

Table 2. Sample sites on Jungfraufirn/Aletsch Glacier (Switzerland) along the trajectory depicted in Figure 10, measured ^{210}Pb activity concentrations and deduced flow rates (Gäggeler and others, 2010)

Sample	Coordinates	Altitude m a.s.l.	^{210}Pb mBq kg^{-1}	Distance to previous site km	Flow rate m a^{-1}
1	643 492/152 890	2925	0.656		
2	645 005/150 898	2751	0.431	2.48	184
3	645 700/150 046	2720	1.269	Excluded, see text	–
4	646 198/149 610	2723	0.314	1.62	159
5	647 853/147 728	2515	0.168	2.41	120
6	648 558/146 565	2485	0.135	1.41	200

Typical uncertainties of ^{210}Pb activity concentrations are ±7%. Coordinates refer to the Swiss coordinate system (Swiss Grid) CH1903/LV03.

^{210}Pb, a potential tool for the determination of net glacier ice flow rates

We tested whether ^{210}Pb surface activity concentrations along a trajectory of the Aletsch Glacier (Switzerland) below the equilibrium line do yield time information on the glacier flow rate. The idea behind this approach is that ^{210}Pb – incorporated in the ice matrix by initial deposition in the accumulation zone and likely being adsorbed on mineral dust particles – is rather immobile. Moreover, it is assumed that ^{210}Pb is not prone to relocation even in the case of percolating meltwater certainly existing in the sampled ablation zone. This seems reasonable based on Avak and others (2018, 2019), showing that lead incorporated in snow and ice is one of the well-preserved trace elements under the conditions of percolating water (~70% preservation). However, later, additional input to the now re-exposed sampled surface in the ablation zone, for example by meltwater from the winter snow and from summer rain is assumed to be entirely removed by run-off. Under such assumptions, the ^{210}Pb activity concentration profile along a downward trajectory should decrease in correspondence to the elapsed time, following the law of decay for ^{210}Pb.

Near-surface samples (after cleaning to remove surface dust layers) of ~10 cm length were taken using a hand-drill device. The sample sites along the trajectory are shown in Figure 10 and are summarized in Table 2, together with the measured ^{210}Pb activity concentrations.

Obviously, the ^{210}Pb values steadily decrease along the trajectory with one exception: in the middle of the Konkordia place, a significantly higher value was measured (sample site 3). Likely the trajectory of ice parcels do not follow the surface at this exceptional site where the Aletsch Glacier is fed from four different sides, from the large firn fields called Jungfraufirn (i.e. the upper part of our trajectory), Ewigschneefeld and Grosser Aletschfirn as well as from the somewhat smaller Grüneggfirn. The value from sample site 3 was therefore discarded. From the ^{210}Pb activity ratio between two sample sites, the known half-life for ^{210}Pb and the distance, the flow rate was deduced, resulting in an average flow rate of 166 m a^{-1} along the entire 7.92 km trajectory.

In a recent paper, Jouvet and Funk (2017) modeled the trajectory of the corpses of mountaineers who disappeared on Aletsch Glacier in 1926. According to their modeling results, the relics were transported parallel to our trajectory between sample sites 4 and 6 (see Table 2) for the time interval from 1985 to 2012. The average flow rate given in Jouvet and Funk (2017) for this section is ~150 m a^{-1}, in surprisingly good agreement with our estimated value of 160 m a^{-1}.

Conclusion

The natural radionuclide ^{210}Pb attached to aerosol particles and deposited on glacier surfaces with fresh snow allows to date glaciers over roughly one century, using its half-life of 22.3 years as a clock. However, the uncertainty is rather large, typically ±5 years for individual samples. This uncertainty is caused mainly by a large variability of ^{210}Pb activity concentrations in individual precipitation events as well as seasonal variability and to lesser extent by counting statistics. Therefore, ^{210}Pb dating should be based on continuous records rather than individual measurements.

In case of glaciers with no or little thinning, the observed chronology of ^{210}Pb activity concentrations as a function of depth follows an exponential decrease. From the slope of the linear fit through the data in a semi-logarithmic plot, the mean annual accumulation rate can be determined. If thinning becomes significant, the decrease of the ^{210}Pb activity concentration as a function of depth is non-linear in such a plot. The measured profile then allows for the determination of thinning as a function of depth.

Some special applications describe that: (i) ^{210}Pb dating – though at a reduced time resolution – can be applicable also for temperate glaciers that are influenced by meltwater; (ii) ^{210}Pb may be used to determine time periods with negative mass balance; (iii) ^{210}Pb measurements of glacier ice core samples in arid regions need to be corrected for sublimation by for example chemical means to deduce total accumulation rates; (iv) the activity concentration ratio between ^{210}Pb and its grand-daughter nuclide ^{210}Po can be used to determine the annual net accumulation rate and finally (v) the ^{210}Pb surface ice activity concentration along a glacier in the ablation zone potentially allows for a determination of glacier flow rates.

Acknowledgements. We highly acknowledge the help of Edith Vogel (University of Bern, Switzerland) and Silvia Köchli (Paul Scherrer Institute, Switzerland) in technical assistance to prepare and measure samples for analysis of ^{210}Pb via ^{210}Po.

References

Appleby PG (2008) Three decades of dating recent sediments by fallout radionuclides: a review. *The Holocene* **18**(1), 83–93. doi: 10.1177/0959683607085598

Appleby PG and Oldfield F (1978) The calculation of lead-210 dates assuming a constant rate of supply of unsupported ^{210}Pb to the sediment. *CATENA* **5**(1), 1–8. doi: 10.1016/S0341-8162(78)80002-2

Avak SE and 7 others (2019) Melt-induced fractionation of major ions and trace elements in an Alpine snowpack. *Journal of Geophysical Research: Earth Surface* **124**, 1647–1657. doi: 10.1029/2019JF005026

Avak SE, Schwikowski M and Eichler A (2018) Impact and implications of meltwater percolation on trace element records observed in a high-Alpine ice core. *Journal of Glaciology* **64**(248), 877–886. doi: 10.1017/jog.2018.74

Balkanski YJ, Jacob DJ, Gardner GM, Graustein WC and Turekian KK (1993) Transport and residence times of tropospheric aerosols inferred from a global three-dimensional simulation of ^{210}Pb. *Journal of Geophysical Research: Atmospheres* **98**(D11), 20573–20586. doi: 10.1029/93JD02456

Baltensperger U, Gäggeler HW, Jost DT, Emmenegger M and Nägeli W (1991) Continuous background aerosol monitoring with the epiphaniometer. *Atmospheric Environment. Part A. General Topics* **25**(3), 629–634. doi: 10.1016/0960-1686(91)90060-K

Crozaz G (1967) *Mise au point d'une methode de datation des glaciers base sur la radioactivite du plomb-210* (PhD thesis). Université Libre de Bruxelles, Faculte des Sciences Appliquees, Belgium.

Crozaz G and Langway Jr CC (1966) Dating Greenland firn-ice cores with Pb-210. *Earth and Planetary Science Letters* **1**, 194–196. doi: 10.1016/0012-821X(66)90067-7

Crozaz G, Picciotto E and de Breuck W (1964) Antarctic snow chronology with Pb-210. *Journal of Geophysical Research* **69**, 2597–2604. doi: 10.1029/JZ069i012p02597

Dadic R, Schneebeli M, Bertler NAN, Schwikowski M and Matzl M (2015) Extreme snow metamorphism in the Allan Hills, Antarctica, as an analogue for glacial conditions with implications for stable isotope composition. *Journal of Glaciology* **61**(230), 1171–1182. doi: 10.3189/2015JoG15J027

Dibb JE (1990) Recent deposition of ^{210}Pb on the Greenland ice sheet: variations in space and time. *Annals of Glaciology* **14**, 51–54. doi: 10.3189/S0260305500008259

Dibb J and Jaffrezo JL (1993) Beryllium-7 and lead-210 in aerosol and snow in the dye 3 gas and aerosol sampling program. *Atmospheric Environment* **27A**(17–18), 2751–2760. doi: 10.1016/0960-1686(93)90307-K

Döscher A, Gäggeler HW, Schotterer U and Schwikowski M (1995) A 130 years deposition record of sulfate, nitrate and chloride from a high-Alpine glacier. *Water, Air and Soil Pollution* **85**, 603–609. doi: 10.1007/BF00476895

Eichler A and 7 others (2000) Glaciochemical dating of an ice core from upper Grenzgletscher (4200 m a.s.l.). *Journal of Glaciology* **46**(154), 507–515. doi: 10.3189/172756500781833098

Feichter J and Crutzen PJ (1990) Parameterization of vertical tracer transport due to deep cumulus convection in a global transport model and its evaluation with ^{222}Radon measurements. *Tellus B: Chemical and Physical Meteorology* **42**(1), 100–117. doi: 10.3402/tellusb.v42i1.15195

Gabrielli P and 40 others (2016) Age of the Mt. Ortles ice cores, the Tyrolean Iceman and glaciation of the highest summit of South Tyrol since the Northern Hemisphere Climatic Optimum. *The Cryosphere* **10**(6), 2779–2797. doi: 10.5194/tc-10-2779-2016

Gäggeler HW (1995) Radioactivity in the Atmosphere. *Radiochimica Acta* **345**, s1. doi: 10.1524/ract.1995.7071.s1.345

Gäggeler HW and 12 others (2011*a*) ^{210}Pb Dating of the Mt. Hutton Ice Core from New Zealand. *Annual Report* 2010, Labor für Radio- und Umweltchemie, Paul Scherrer Institut, p. 64.

Gäggeler HW and 12 others (2011*b*) ^{210}Pb Dating of the Baker and Annette Ice Cores from New Zealand, *Annual Report* 2010, Labor für Radio- und Umweltchemie, Paul Scherrer Institut, p. 65.

Gäggeler HW, Jost DT, Baltensperger U, Schwikowski M and Seibert P (1995) Radon and thoron decay product and ^{210}Pb measurements at Jungfraujoch, Switzerland. *Atmospheric Environment* **29**(5), 607–616. doi: 10.1016/1352-2310(94)00195-Q

Gäggeler HW, Szidat S, Vogel E, Tobler L and Boss H (2010) Is ^{210}Pb suited for the determination of glacier flow rates?. *Annual Report* 2009, Labor für Radio- und Umweltchemie, Paul Scherrer Institut, p. 66.

Gäggeler HW, Tobler L and Vogel E (2009) Accumulation rates determined from radioactive disequilibrium between ^{210}Po and ^{210}Pb. *Annual Report* 2008, Labor für Radio- und Umweltchemie, Paul Scherrer Institut, p. 34.

Gäggeler H, von Gunten HR and Nyffeler U (1976) Determination of ^{210}Pb in lake sediments and in air samples by direct gamma-ray measurement. *Earth and Planetary Science Letters* **33**(1), 119–121. doi: 10.1016/0012-821X(76)90164-3

Gäggeler H, von Gunten HR, Rössler E, Oeschger H and Schotterer U (1983) ^{210}Pb-dating of cold alpine firn/ice cores from Colle Gnifetti, Switzerland. *Journal of Glaciology* **29**(101), 165–177. doi: 10.3189/S0022143000005220

Ginot P (2001) *Glaciochemical study of ice cores from Andean glaciers* (PhD thesis). Dept. Chem. and Biochem., Univ. of Bern, Switzerland.

Ginot P and 7 others (2002) Potential for climate variability reconstruction from Andean glaciochemical records. *Annals of Glaciology* **35**, 443–450. doi: 10.3189/172756402781816618

Ginot P, Kull C, Schotterer U, Schwikowski M and Gäggeler HW (2006) Glacier mass balance reconstruction by sublimation induced enrichment of chemical species on Cerro Tapado (Chilean Andes). *Climate of the Past* **2**(1), 21–30. doi: 10.5194/cp-2-21-2006

Goldberg ED (1963) Geochronology with ^{210}Pb: radioactive dating. Proceedings of the Symposium on Radioactive Dating Held by the International Atomic Energy Agency in Cooperation with the Joint Commission on Applied Radioactivity, Athens, Greece, November 1962, pp. 121–131.

Haefeli R (1961) Contribution to the movement and the form of ice sheets in the Arctic and Antarctic. *Journal of Glaciology* **3**(30), 1133–1151. doi: 10.3189/S0022143000017548

Herren PA and 6 others (2013) The onset of Neoglaciation 6000 years ago in western Mongolia revealed by an ice core from the Tsambagarav mountain range. *Quaternary Science Reviews* **69**, 59–68. doi: 10.1016/j.quascirev.2013.02.025

Hötzl H, Rosner G and Winkler R (1983) Report Radionuclide concentrations in ground level air and precipitation in South Germany from 1976 to 1982, Gesellschaft für Strahlen- und Umweltforschung mbH, München, *GSF-Bericht S*-956, ISSN 0721-1694.

Hou SG and 7 others (2018) Age ranges of the Tibetan ice cores with emphasis on the Chongce ice cores, western Kunlun Mountains. *The Cryosphere* **12**(7), 2341–2348. doi: 10.5194/tc-12-2341-2018

Jouvet G and Funk M (2017) Modelling the trajectory of the corpses of mountaineers who disappeared in 1926 on Aletschgletscher, Switzerland. *Journal of Glaciology* **60**(220), 255–261. doi: 10.3189/2014JoG13J156

Kang S and 10 others (2015) Dramatic loss of glacier accumulation area on the Tibetan Plateau revealed by ice core tritium and mercury records. *The Cryosphere* **9**(3), 1213–1222. doi: 10.5194/tc-9-1213-2015

Knüsel S and 8 others (2003) Dating of two nearby ice cores from the Illimani, Bolivia. *Journal of Geophysical Research* **108**(D6), 4181. doi: 10.1029/2001JD002028

Kuroda PK, Daniel PY, Nevissi A, Beck JN and Meason JL (1978) Atmospheric residence times of strontium-90 and lead-210. *Journal of Radioanalytical Chemistry* **43**(2), 443–450. doi: 10.1007/BF02519505

Lee HN and Feichter J (1995) An intercomparison of wet precipitation scavenging schemes and the emission rates of ^{222}Rn for the simulation of global transport and deposition of ^{210}Pb. *Journal of Geophysical Research: Atmospheres* **100**(D11), 23253–23270. doi: 10.1029/95JD01732

Marx SK, Kamber BS and McGowan HA (2005) Estimate of Australian dust flux into New Zealand: quantifying the eastern Australian dust plume pathway using trace element calibrated ^{210}Pb as a monitor. *Earth and Planetary Science Letters* **239**, 336–351. doi: 10.1016/j.epsl.2005.09.002

Mason B and Moore CB (1982) *Principles of Geochemistry*, 4th Edn., New York: Wiley & Sons.

Moore HE, Poet SE and Martell EA (1973) ^{222}Rn, ^{210}Pb, ^{210}Bi, and ^{210}Po profiles and aerosol residence times versus altitude. *Journal of Geophysical Research* **78**(30), 7065–7075. doi: 10.1029/JC078i030p07065

Morse DL and 7 others (1999) Accumulation rate measurements at Taylor Dome, East Antarctica: techniques and strategies for mass balance measurements in polar environments. *Geografiska Annaler. Series A. Physical Geography* **81**(4), 683–694. doi: 10.1111/1468-0459.00106

Nijampurkar VN, Bhandari N, Borole DV and Bhattacharya U (1985) Radiometric chronology of Changme-Khangpu glacier, Sikkim. *Journal of Glaciology* **31**(107), 28–33. doi: 10.3189/S0022143000004950

Nijampurkar VN and Rao DK (1993) Snow and Glacier Hydrology. Proceedings of the Kathmandu Symposium, November 1992, Katmandu, Nepal, IAHS Publ. no. 218, pp. 355–369.

Olivier S and 7 others (2006) Temporal variations of mineral dust, biogenic tracers, and anthropogenic species during the past two centuries from Belukha ice core, Siberian Altai. *Journal of Geophysical Research: Atmospheres* **111**(D5), D05309. doi: 10.1029/2005JD005830

Pavlova PA and 5 others (2015) Polychlorinated biphenyls in a temperate Alpine Glacier: 1. Effect of percolating meltwater on their distribution in glacier ice. *Environmental Science & Technology* **49**(24), 14085–14091. doi: 10.1021/acs.est.5b03303

Peters AJ, Gregor DJ, Wilkinson P and Spencer C (1997) Deposition of Pb-210 to the Agassiz Ice Cap, Canada. *Journal of Geophysical Research: Atmospheres* **102**(D5), 5971–5978. doi: 10.1029/96JD01843

Picciotto E, Crozaz G, Ambach W and Eisner H (1967/1968) Lead-210 and strontium-90 in an Alpine glacier. *Earth and Planetary Science Letters* **3**, 237–242. doi: 10.1016/0012-821X(67)90043-X

Pinglot JF and 13 others (2003) Ice cores from Arctic sub-Polar glaciers: chronology and post-depositional processes deduced from radioactivity measurements. *Journal of Glaciology* **49**(164), 149–158.

Rangarajan C, Madhavan R and Gopalakrishnan SS (1986) Spatial and temporal distribution of lead-210 in the surface layers of the atmosphere. *Journal of Environmental Radioactivity* **3**(1), 23–33.

Sanak J and Lambert G (1977) Lead 210 or climatic changes at South Pole? *Geophysical Research Letters* **4**(9), 357–359. doi: 10.1029/GL004i009p00357

Schläppi M (2010) *Accumulation rates and chemical composition of precipitation derived from Pio XI ice core, Southern Patagonia Icefield* (PhD thesis). Dep. Chem. and Biochem., Univ. of Bern, Switzerland.

Schotterer U and 7 others (1977) Isotope measurements on firn and ice cores from Alpine glaciers. Proceedings of a symposium held during the XVI Assembly of the International Union of Geodesy and Geophysics at Grenoble, August–September 1975, Grenoble, France, pp. 232–236.

Steinmann P and 6 others (2015) Report Umweltradioaktivität und Strahlendosen in der Schweiz, Ergebnisse 2014, Chapter 4.1, BAG (Bundesamt für Gesundheit), Switzerland (in German and French).

Suzuki T, Kamiyama K, Furukawa T and Fujii Y (2004) Lead-210 profile in firn layer over Antarctic ice sheet and its relation to the snow accumulation environment. *Tellus B: Chemical and Physical Meteorology* **56**(1), 85–92. doi: 10.3402/tellusb.v56i1.16403

Turekian KK, Nozaki Y and Benninger LK (1977) Geochemistry of atmospheric radon and radon products. *Annual Review of Earth and Planetary Sciences* **5**(1), 227–255. doi: 10.1146/annurev.ea.05.050177.001303

Vimeux F and 7 others (2008) A promising location in Patagonia for paleoclimate and paleoenvironmental reconstructions revealed by a shallow firn core from Monte San Valentín (Northern Patagonia Icefield, Chile). *Journal of Geophysical Research* **113**, D16118. doi: 10.1029/2007JD009502

Vincent C, Vallon M, Pinglot JF, Funk M and Reynaud L (1997) Snow accumulation and ice flow at Dôme du Goûter (4300 m), Mont Blanc, French Alps. *Journal of Glaciology* **43**(145), 513–521. doi: 10.3189/S0022143000035127

von Gunten HR, Rössler E and Gäggeler H (1982) Dating of ice cores from Vernagtferner (Austria) with fission products and lead-210. *Zeitschrift für Gletscherkunde und Glazialgeologie* **18**(1), 37–45, hdl:10013/epic.38455.d001.

Wang C and 7 others (2014) ^{210}Pb Dating of the Miaoergou ice core from the eastern Tien Shan, China. *Annals of Glaciology* **55**(66), 105–110. doi: 10.3189/2014AoG66A151

Wedepohl H (1995) The composition of the continental crust. *Geochimica et Cosmochimica Acta* **59**(7), 1217–1232. doi: 10.1016/0016-7037(95)00038-2

Wendl IA, Eichler A, Isaksson E, Martma T and Schwikowski M (2015) 800-year ice-core record of nitrogen deposition in Svalbard linked to ocean productivity and biogenic emissions. *Atmospheric Chemistry and Physics* **15**(13), 7287–7300. doi: 10.5194/acp-15-7287-2015

Zemp M and 38 others (2015) Historically unprecedented global glacier decline in the early 21st century. *Journal of Glaciology* **61**(228), 745–762. doi: 10.3189/2015JoG15J017